Task Ambient Air Conditioning System with Natural Ventilation for High Rise Office Building
(Part 2: Measurement of Natural Ventilation Rate and CFD Analysis using Measured Data)

H. Kotani[1], K. Sagara[1], T. Yamanaka[1], M. Kuise[1], M. Yamagiwa[2], S. Horikawa[3] and T. Ushio[3]

[1] Osaka University, 2-1 Yamadaoka, Suita Osaka 565-0871, Japan
email: kotani@arch.eng.osaka-u.ac.jp http://www.arch.eng.osaka-u.ac.jp
[2]THE KANSAI ELECTRIC POWER CO., INC., 3-6-16 Nakanoshima, Kita-ku Osaka 530-8270, Japan
[3] NIKKEN SEKKEI LTD., 4-6-2 Koraibashi, Chuo-ku Osaka 541-8528, Japan

Summary: Detailed discussions of the natural ventilation measurement follow the previous paper (Part 1). Inflow and outflow distribution by each natural ventilation opening are calculated for sixteen outside wind directions. In case that the outside wind direction is around southwest, calculated values are similar to the measured values. CFD analysis using these measured data was conducted as well. The condition where a west wind of 4.5 m/s was blowing was reproduced and it was confirmed by CFD that the outdoor air reaches a point approximately 15 m away from the west end of the room.

Keywords: *task ambient air conditioning system, natural ventilation, CFD analysis*
Category: *indoor climate specific designs, ventilation, innovative technologies and solutions*

1 Introduction

Part 1 of this paper [1] showed results of the macroscopic evaluation of the natural ventilation performance and the thermal environment of the task ambient air conditioning with natural ventilation based on the measurement results. This part of the paper shows the natural ventilation performance in detail selecting a period when the natural ventilation is stable. This paper also deals with a CFD analysis using measured data as the boundary condition and reproduces the temperature and air velocity distributions in the whole office room.

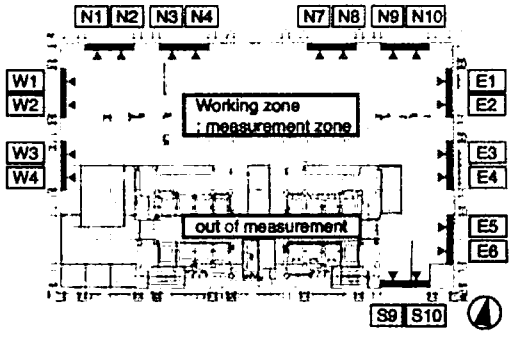

Fig. 1 Plan of office floor and natural ventilation openings

2 Measurement of natural ventilation rate

The measurement was conducted at the same office room of the 30th story (GL +131.63 m) of the same high rise office building as Part 1 of this paper. Detailed measurements of natural ventilation rate were made from 13:50 to 17:50 on 23rd April, 2005 while twenty natural ventilation openings (see Fig.1) were kept open and the task air conditioning was operated. The omni-directional constant temperature anemometer was set at the natural ventilation opening as shown in Fig.2. Measurement frequency was 10 Hz and the judgment of inflow and outflow at the opening was conducted by continuous observation of the tuft set at the opening. Natural ventilation rates of fifteen openings except W4, E5, E6, S9 and S10 in Fig.1 were investigated.

Fig.3 shows the wind velocity variations at every natural ventilation openings from 14:00 to 17:50. West-side openings of W1, W2 and W3 work mainly as inflow openings, and others work as outflow inflow

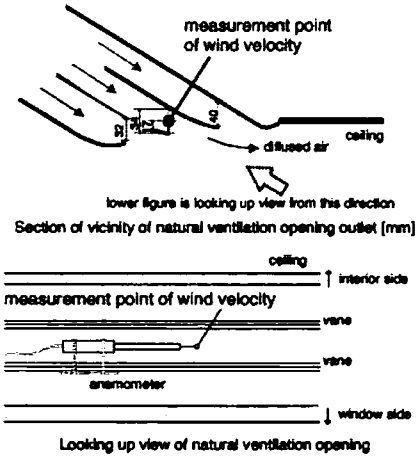

Fig.2 Velocity measurement at each natural ventilation opening

openings, because the outdoor wind direction was openings. N7 to N10, El and E2 sometimes works as changing from southwest to west, sometimes to north. Wind direction data at Osaka weather station (Osaka District Meteorological Observatory: GL+33m) was southwest (SW) from 14:00 to 16:00 and west-southwest (WSW) from 16:00 to 18:00. Wind velocity at the openings during measuring period decreased according with time, this tendency corresponded to the outdoor wind velocity data at Osaka weather station as well. Lower figure of Fig.3 shows the enlargement of five minutes from 14:00 to 14:25 when the natural ventilation was stable and its rate was relatively large. During this period, west-side openings of Wl, W2 and W3 worked as inflow openings at the wind velocity of 1.6 to 3.3 m/s, and others worked as outflow openings at 0.4 to 1.9 m/s. In the following discussions, this period is selected for the evaluation of the ventilation performance. Fig.4 shows the flow rate at each opening calculated by multiplication above-mentioned wind velocity by the opening area. It was seen that flow rates at the inflow openings (Wl to W3) are larger than those at the outflow openings (Nl to N10 and El to E4). At the outflow openings, flow rates at the north-side openings are larger than those of eastside openings, but the difference of outflow opening location makes some flow rate difference.

Table 1 shows the calculated result of the air change rate of whole office room. Two volumes were used for calculation here, that is the volume excluding or including southeast zone where is surrounded by E4 to E6, S9 and S10 (see Fig.l). The flow rate balance was not achieved because the inflow rate at W4, S9 and S10 seems to be large where the flow rate measurement was not conducted. The air change rate was about 6 to 7 times/h on the outflow side. This results show that these natural ventilation openings worked very well.

3 Calculation of natural ventilation rate

Inflow and outflow distribution by each natural ventilation opening were calculated for sixteen outside wind directions using wind pressure coefficients (Cp) obtained by wind tunnel tests. For the comparison with the measured flow rate (see Fig.4), the outdoor wind velocity of 5 minutes from 14:20 to 14:25 was assumed to be 4.5 m/s at Osaka weather station (GL+33m) from its observed data of 14:00 and 15:00. One-fourth power low of atmospheric boundary layer was also assumed to use Cp data. It should be noted that Cp was measured at the 23rd floor (GL+100m) in the wind tunnel model, but the actual measurement was conducted at the 30th floor (GL+131.63m), so there is a little difference. The temperature-induced ventilation between outdoor and indoor temperature difference was neglected and only the wind-induced ventilation rate was calculated.

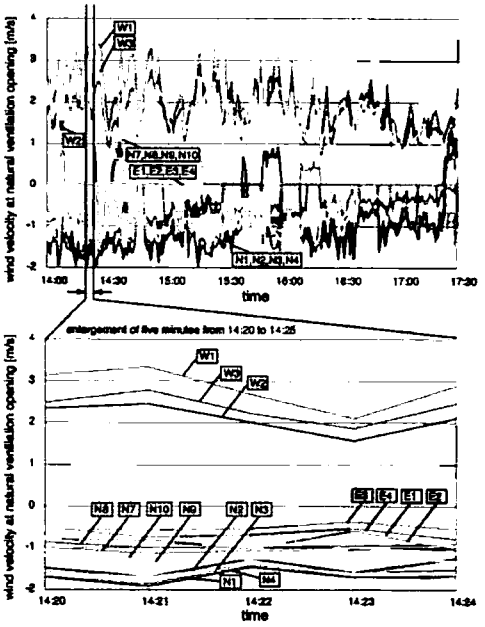

Fig.3 Wind velocity variations at natural ventilation openings

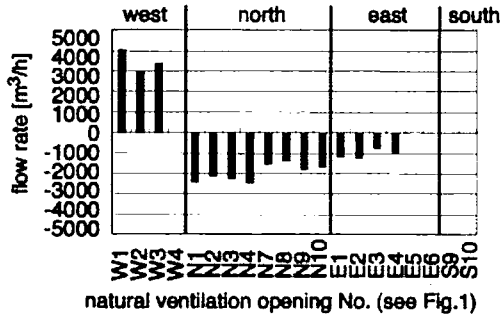

Fig.4 Measurement result of natural ventilation rate (14:20 to 14:25)

Table 1 Calculated inflow and outflow rate (14:20 to 14:25)

	flow rate [m3/h]	air change rate [ACH]	
		(1)	(2)
inflow	10.455	3.6	3.0
outflow	-19.785	-6.8	-5.7
balance	-9.330	-3.2	-2.7

(1) Air change rate using working zone volume excluding southeast zone.
floor area: 1,037m^2, volume: 2,903m^3

(2) Air change rate using working zone volume including southeast zone.
floor area: 1,232m^2, volume: 3,448m^3

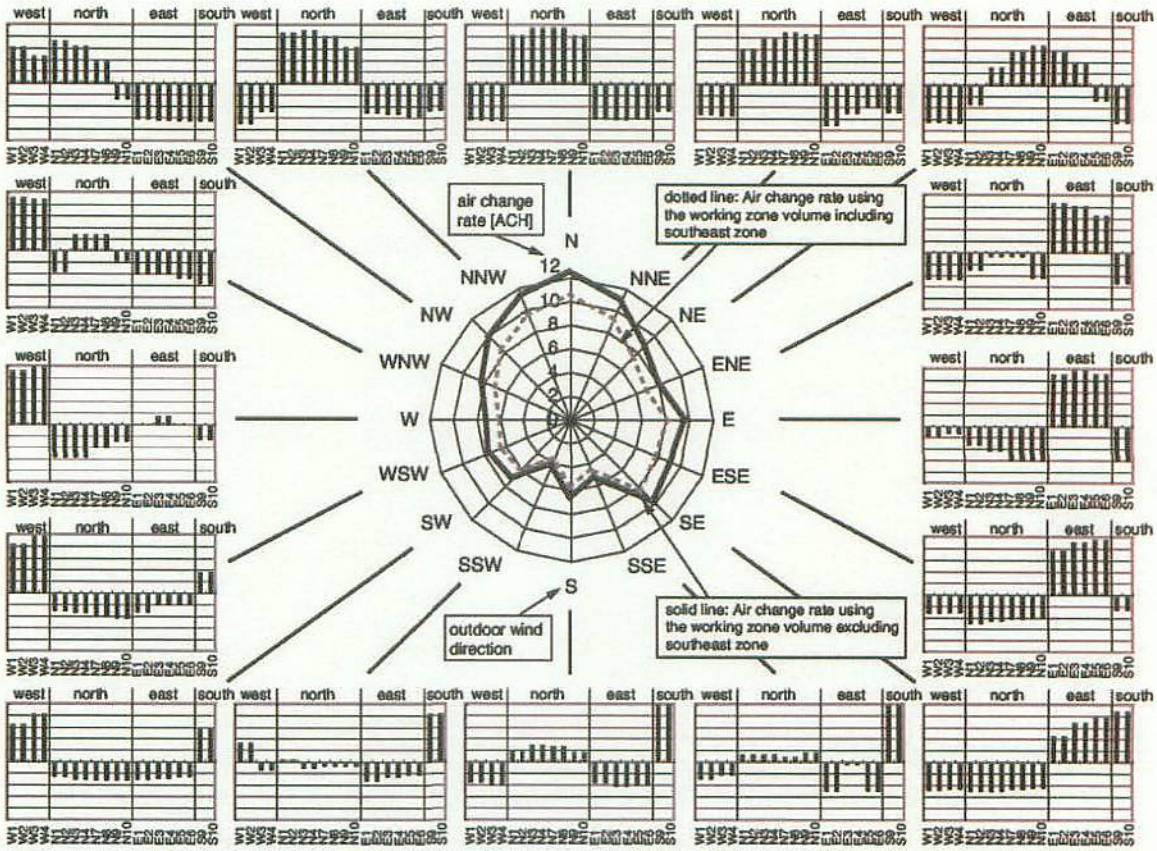

Fig.5 Calculation results of natural ventilation rate at each opening for 16 outdoor wind directions
(centeral fig.: ak change rate for each wind direction, surrounding: inflow and outflow rate of each ventilation opening at each outdoor wind direction.)

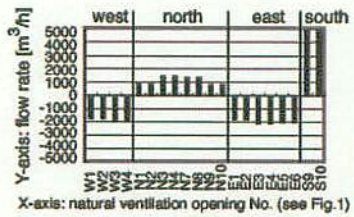

This figure is a case noted 'S'.
* 'S' means that the outdoor wind direction is south.
* Values of bar show the inflow and outflow rate at each natural ventilation opening
* Y-axes of every figures are the same as -5,000 to 5000 [m^3/h]
* X-axes are the natural ventilation opening number (see Fig.1).

In this case:

8 openings at the north-side (N1 to N10) and 2 openings at the south-side (S9 and S10) work as inflow openings, and 4 openings at the west-side (W1 to W4) and 6 openings at the east-side (E1 to E6) work as outflow openings.

Fig.6 How to read each figure in Fig.5

Fig.5 shows the calculation results of the natural ventilation rate at each opening (surrounding figure) and the air change rates (central figure) for 16 outdoor wind directions. Fig.6 explains how to read the surrounding each figure of Fig.5. The air change rates for the wind direction of around south (SSW, S and SSE) are small because there are little south-side openings (only S9 and S10). For the wind direction of around north (NNW, N and NNE), the air change rates are about two times as large as the case of south wind. It can be said that enough air change rates are expected for almost all wind direction except the wind direction of around south. The prevailing wind directions in Osaka are SW to W at spring season and N to NE at fall season. The natural ventilation performance of this building for these wind directions is expected to be very high.

In case that the outside wind direction is around southwest (SW) to west-southwest (WSW), calculated flow rates at each opening are very similar to the measured values (compare with Fig.4). This corresponded to the fact that the wind direction data at Osaka weather station was southwest (SW) from 14:00 to 15:00. There are some differences of Cp and measurement errors, but this result can also guarantee the accuracy of the wind velocity measurement at each natural ventilation opening.

4 CFD analysis of office room using measured data

The accuracy of measured flow rates at natural ventilation openings were checked by the previous chapter. Therefore CFD analysis was conducted for office room using these measured values of the flow rates and temperatures at natural ventilation openings when the outdoor wind velocity is 4.5 m/s. The north

part of the office room (see Fig.l) was modeled as shown in Fig.7. Each natural ventilation opening was settled at the ceiling with its height of 10cm and the outdoor air was diffused horizontally from this opening when the opening works as inflow opening. Wind velocities calculated from the measured flow rate (see Fig.4) are defined at the natural ventilation opening as boundary conditions of CFD. The other measured values of task floor outlets and internal heat generation rate are used as boundary conditions of CFD as well. Fig.8 shows the detailed figure with the mesh system of CFD. The size of most meshes is 20x20x20cm, and some meshes around natural ventilation openings and floor outlets are sized as 10x10x10cm. Internal heat load of person was simulated by the black lamp of 60W in the actual measurement, but CFD analysis used the rectangular heating box of 60W on the chair as shown in Fig. 8. Table 2 summarizes the outline of CFD analysis, boundary conditions of flow rate and boundary conditions of the internal heat load.

Fig. 9 shows the calculated velocity distribution inside the office room. The outdoor air entering from the west-side natural ventilation opening was observed to flow along the ceiling surface by 'Coanda effect' and gradually dropped as the flowing air temperature was lower than the room temperature, but did not drop down to the occupancy zone within 15 meters from the west-side wall. As north-side natural ventilation openings worked as outflow openings, outdoor air flowed to north-side zone of the office room and high velocities were obtained at the plane of Fl+950mm. High wind velocities near the south-side wall seemed to be caused by the outdoor air from W3 (see Fig.l) flowed along the south-side wall. This airflow pattern was also observed by the flow visualization at the actual measurement. Wind velocities were very low at the central and eastside zone of the office room.

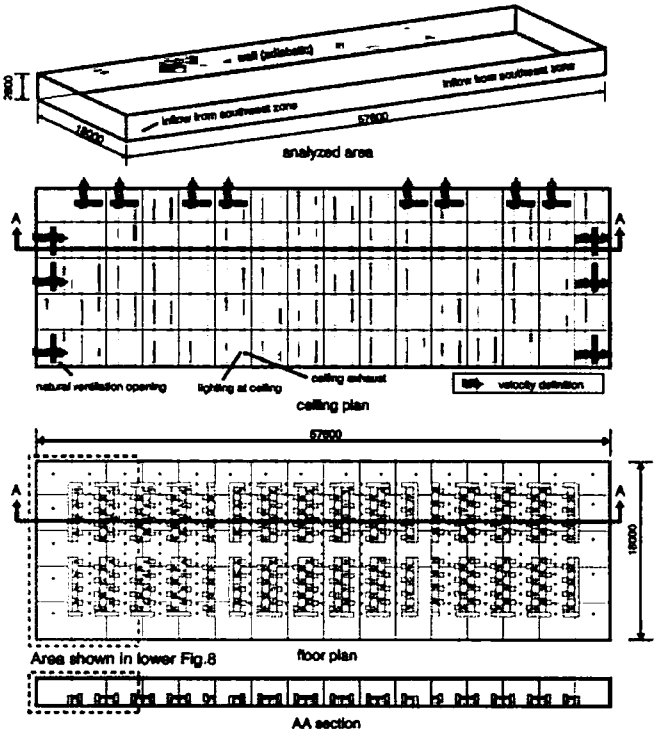

Fig.7 Office room model for CFD (upper fig: plan, lower: AA section)

Table 2 CFD conditions

Outline		
code	FLUENT 6.1	
turbulence model	standard k-ε	
analyzed area	18 x 57.6 x 2.8 [m]	
number of meshes	90 x 288 x 15	
differential scheme	QUICK	
wall boundary condition	standard log-law, adiabatic	
Boundary conditions of flow rate		
	flow rate,	number
floor outlet	110 m³/h, 23 degC	206
ceiling exhaust	78.6 m³/h	288
natural ventilation	Velocity definition derived from 18.8 degC (Osaka weather station)	
Boundary conditions of internal heat load		
source	each heat load	number
black lamp	60 W	104
laptop pc	30 W	208
lightning at ceiling	32 W 60 % to setting positions 40 % to floor, desks and walls	288
total		

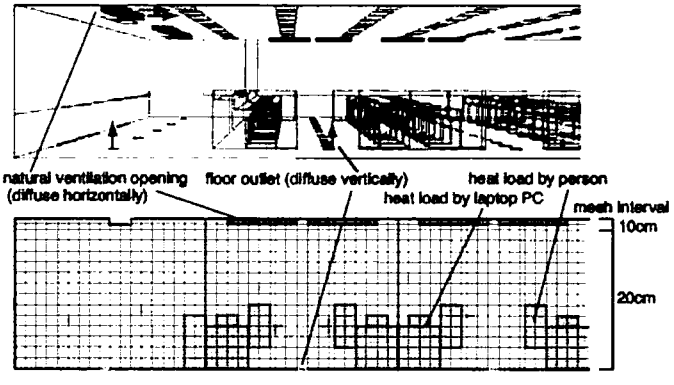

Fig.8 Detailed figure for CFD

Calculated temperature distribution inside the office room shown in Fig. 10 can be explained by above-mentioned outdoor airflow pattern from natural ventilation openings as well. Outdoor airflow from the west-side opening to the north-side one caused the low temperature zone at the northwest zone of the room, and temperatures were higher at the central and eastside zone of the room. Low temperature near the south-side wall was caused by the outdoor air from W3 opening. High temperature at the southeast zone was due to the air with high temperature that comes from southeast zone. In the same way, the airflow from the southwest zone where the airflow rates were not measured was considered as the boundary conditions of CFD. Future discussions are needed for these boundary conditions.

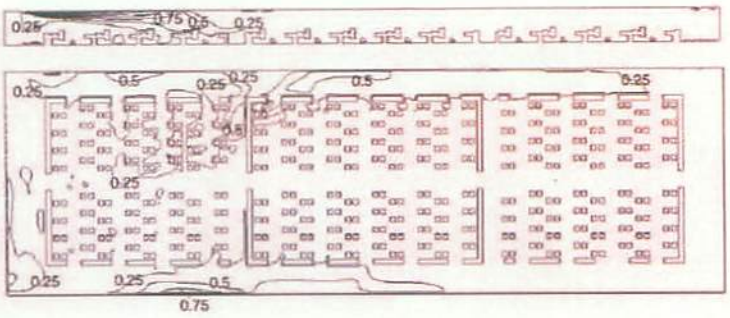

Fig.9 Velocity distribution [m/s] (upper fig.: AA section, lower: plan at FL+950mm)

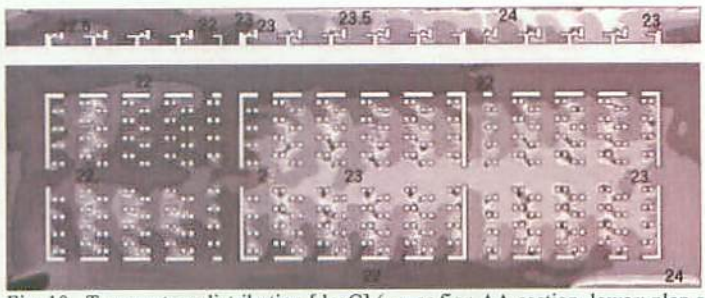

Fig. 10 Temperature distribution [degC] (upper fig.: AA section, lower: plan at FL+950mm)

The airflow pattern mentioned above was also explained in Fig. 10 that outdoor air flowed mainly from west-side openings to north-side zone of the office room with its drop to the occupancy zone. Fig. 12 shows the velocity vector (upper figure) and velocity distribution (lower figure) at the zone of 1/3 from the west-side wall, that is the part of Fig.9. The tendency was seen obviously that the outdoor air from the west-side natural ventilation opening flowed along the ceiling surface and gradually dropped at the certain distance from the wall. Velocity vectors caused by the floor outlet were also observed. Fig. 13 shows the flow visualization photos for understanding the airflow pattern from the natural ventilation opening. Photos were sized to almost the same scale as Fig. 12. Visualization was made for the north-side ventilation opening (CFD was made for west-side opening). Wind velocity at the opening was about 1.0 to 1.5 m/s and the inflow temperature was 16.6 degC (2.4 m/s and 18.8 degC in CFD). The boundary conditions of CFD and visualization are different, but the airflow pattern agreed well. Fig. 14 compares the temperature distribution inside office room between measurement and CFD analysis at the height of FL+950mm. General tendency was similar that the temperature is low at west-side zone and higher temperature is seen in east-side zone. However the measured temperature increment about 3.0 degC from west to east was not reproduced by CFD analysis of which temperature increment was about 1.0 to 2.0 degC. There might be some reasons of this difference, for instance the heat storage by floor, ceiling or office furniture, errors in the natural ventilation rate measurement as the boundary condition of CFD, errors in other boundary conditions of CFD and so on.

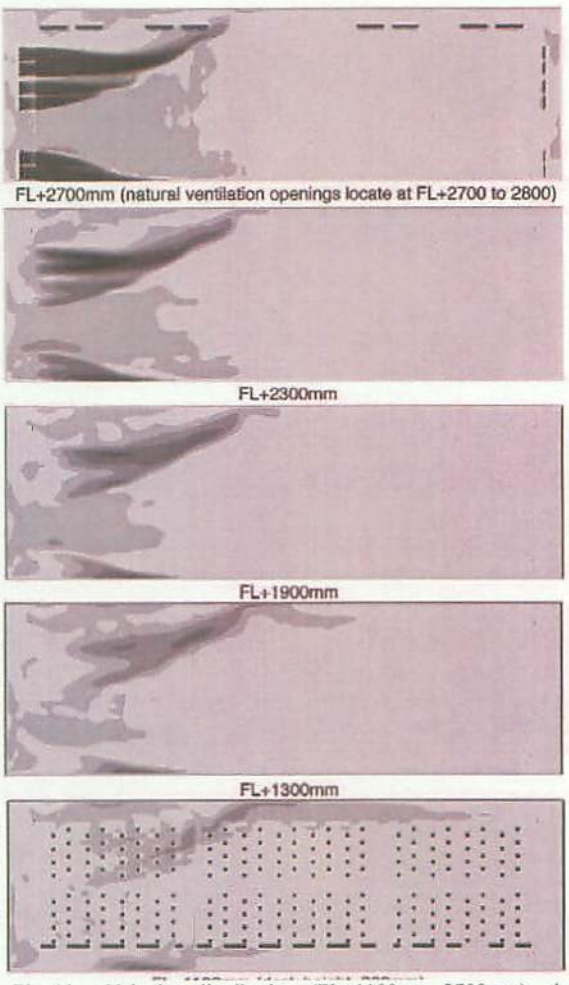

Fig. 11 Velocity distribution (FL+1100 to 2700mm), the interval of contour line: 0.25 m/s

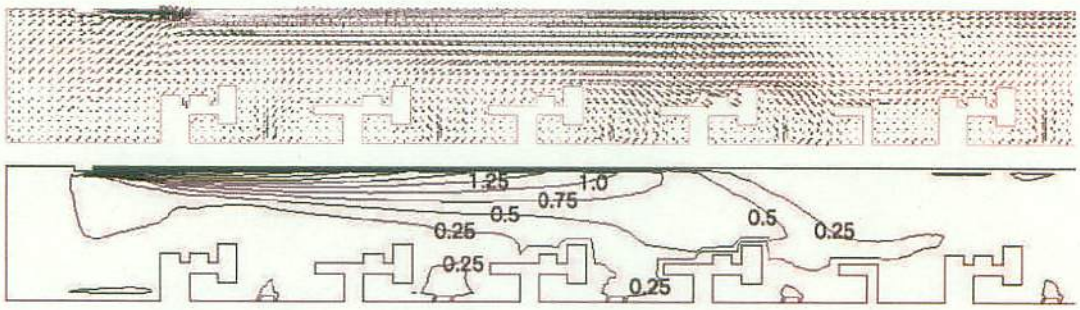

Fig. 12 Velocity vector (upper fig.) and velocity distribution [m/s] (lower) at the zone of 1/3 from the west-side wall.

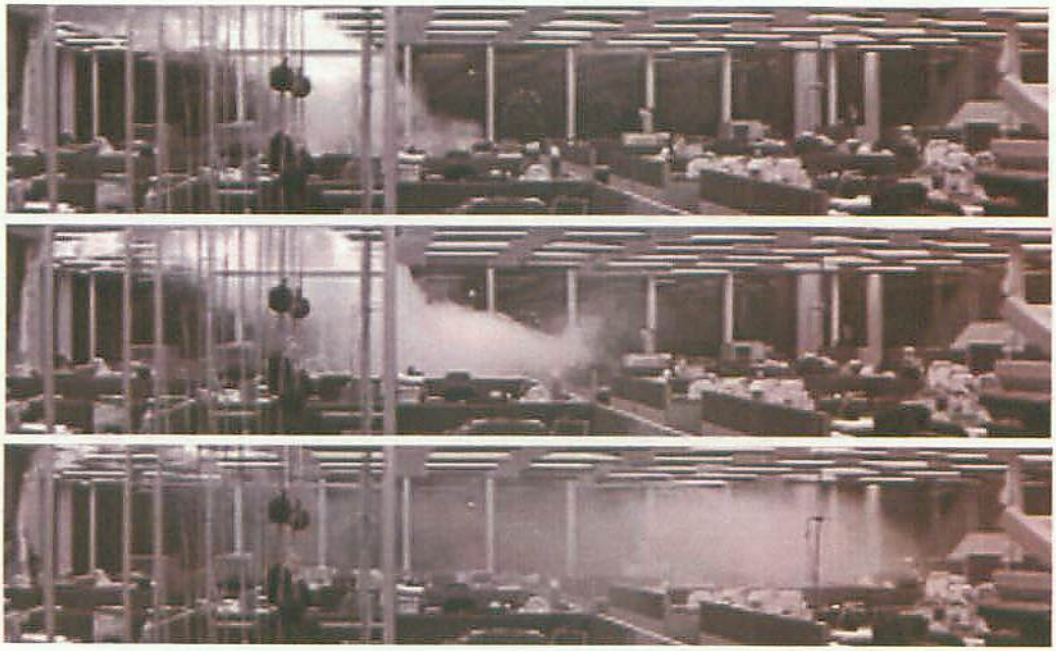

Fig. 13 Flow visualization photos (from above; 12 sec., 24 sec. and 48 sec. after smoke generation at natural ventilation opening)

5 Conclusion

Detailed discussions of the natural ventilation measurement were made. Results of calculation of natural ventilation rate for sixteen outdoor wind direction showed that the natural ventilation openings work very well with enough air change rate of office room to the prevailing wind direction in Osaka. Calculations also guaranteed the accuracy of the natural ventilation rate measurements. CFD analysis was conducted to know the detailed airflow pattern inside a room. As a result, basic airflow pattern caused by natural ventilation was clarified and showed the good agreement with the flow visualization result.

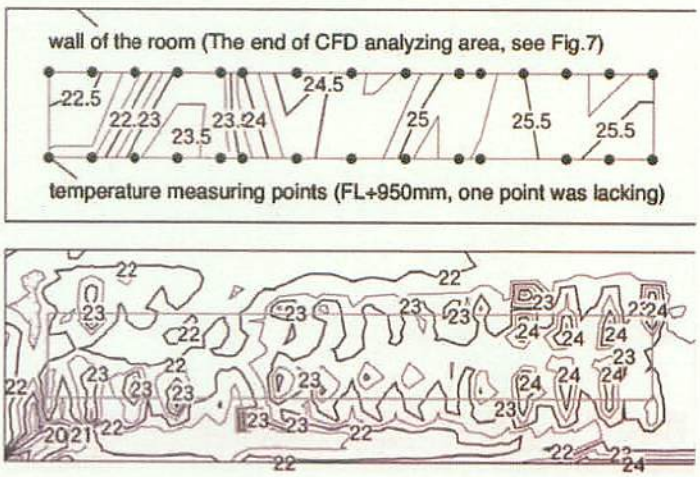

Fig. 14 Temperature distribution [degC] (upper fig.: measurement, lower: CFD)

Acknowledgement

The authors would like to thank Ms. Eunsu Lim, Mr. Tatsuya Yamashita and members of authors' research group for their supports in carrying out measurements.

References

[1] T.Ushio et al.: Task Ambient Air Conditioning System with Natural Ventilation for High Rise Office Building(Part 1), *Healthy Buildings 2006*, Lisboa, 2006.